531

Reprinted from "Collapse"
edited by J. M. T. Thompson and G. W. Hunt

3

Buckle propagation on a beam on a nonlinear elastic foundation

E. CHATER AND J. W. HUTCHINSON
Division of Applied Sciences, Harvard University, Cambridge, MA 02138, USA

K. W. NEALE
Department of Civil Engineering, University of Sherbrooke, Sherbrooke, Quebec, Canada

3.1 Introduction

Certain structures have the tendency to propagate a buckle once one is initiated. Perhaps the most important example is buckle propagation along an undersea pipeline (Palmer & Martin, 1975). Buckle propagation along a pipeline involves large deflections and plastic deformation. A detailed theoretical analysis of the propagation process in the pipeline problem has not yet been performed, although important related theoretical and experimental studies have been carried out (e.g. Kyriakides & Babcock, 1980; 1981). In this paper we study buckle propagation in a simple model system with the aim of elucidating some of the general features of buckle propagation in elastic structures. A feature common to both the pipeline and our model problem is that once initiated the buckle can spread at a load substantially below the initial buckling load of the perfect structure. It is this aspect of the phenomenon which renders it of some practical significance.

The model is a linear elastic beam resting on a nonlinear elastic foundation with a stiffness per unit length of $k(w)$ where w is the lateral deflection. The beam is subject to a uniform lateral load P as depicted in Fig. 3.1. The restoring force per unit length of the foundation, $F = k(w)w$, is assumed to have the general form shown in Fig. 3.1 with F rising to a peak, F_{max}, falling to a local minimum, F_{min}, and then increasing steadily with further compression.

At any load per unit length P which falls between F_{min} and F_{max}, a straight beam has three possible static equilibrium displacements, w_A, w_M and w_B, with the intermediate deflection w_M being unstable. We will suppose $F_{min} < P < F_{max}$ and we will begin by looking for buckling modes such as that shown in Fig. 3.1 where the beam has a straight collapsed section behind the transition region with deflection w_B as $x \to -\infty$ and an uncollapsed straight section with $w = w_A$ ahead of the transition as $x \to +\infty$. We will show that there exists only one load P^* corresponding to a mode of this type, and that load falls roughly halfway between F_{min} and F_{max}. Furthermore, quasi-static, steady-state propagation of the mode along the beam is possible at the load P^*. That is, if inertia is neglected, continuing buckling can take place with the mode assuming a fixed profile which simply translates down the beam.

We will then consider the initiation process by analyzing the spread of the zone of collapse from an initially weak region of the foundation. As the buckle spreads and begins to propagate, it approaches the steady-state mode shape as the load approaches P^*. Finally, we end the paper with a brief study of the effect of inertia on dynamic steady-state propagation.

3.2 Quasi-static, steady-state propagation

The equation governing the deflection of the infinite beam is

$$EI\frac{d^4 w}{dx^4} + k(w)w = P, \tag{1}$$

where EI is the uniform bending stiffness. We look for solutions to (1) for $P = P^*$ between F_{min} and F_{max} such that

$$\left.\begin{aligned} w &\to w_A \quad \text{as} \quad x \to +\infty \\ w &\to w_B \quad \text{as} \quad x \to -\infty, \end{aligned}\right\} \tag{2}$$

where

$$k(w_A)w_A = k(w_B)w_B = P^*. \tag{3}$$

Fig. 3.1. Beam on nonlinear elastic foundation.

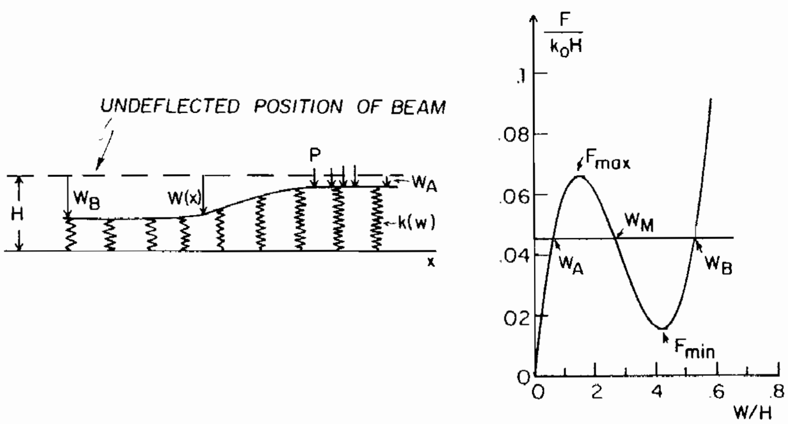

To obtain a third equation relating P^*, w_A and w_B, multiply (1) by dw/dx and integrate with respect to x from $-\infty$ to $+\infty$ with the result

$$\int_{-\infty}^{\infty} EI \frac{d^4w}{dx^4}\frac{dw}{dx}dx + \int_{-\infty}^{\infty} k(w)w\frac{dw}{dx}dx = \int_{-\infty}^{\infty} P^* \frac{dw}{dx}dx. \tag{4}$$

Assuming that (2) pertains and that the derivatives of w vanish as $x \to \pm\infty$, one finds, using integration by parts, that the first term in (4) is zero. The remaining condition can be rewritten as

$$\int_{w_A}^{w_B} k(w)w\, dw = P^*(w_B - w_A). \tag{5}$$

The term on the left in (5) is just the work per unit length needed to deform the foundation from w_A to w_B. Equation (5) with (3) has the graphical solution shown in Fig. 3.2, i.e. the area under the force–deflection curve between w_A and w_B must be equal to the area of the rectangle with height P^* and width $w_B - w_A$. Or, equivalently, the areas of $\mathscr{R}_1$ and $\mathscr{R}_2$ must be equal. In the context of phase transformations, James (1979) refers to the horizontal line in Fig. 3.2 as the 'Maxwell line' after Maxwell (1875) who noted the relevance of this graphical solution to certain coexisting phases.

For a force–deflection curve such as that shown in Fig. 3.2 there is only one load P^* at which this type of collapse mode can exist. Furthermore, the mode can undergo quasi-static propagation along the beam at load P^*. This will be made clearer in the next section when we take

Fig. 3.2. Graphical solution for load P^* for quasi-static, steady-state buckle propagation ($\mathscr{R}_1 = \mathscr{R}_2$).

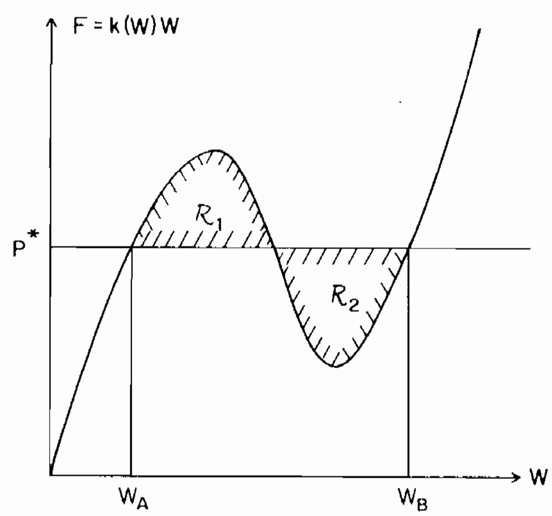

the quasi-static limit of a steady-state propagating solution which includes inertia. Here we note that if $w(x)$ is a solution to (1) then so is $w(x-a)$, corresponding to a shift of the buckle to the right (or left) by any amount a. For steady propagation of the buckle in the positive x-direction at constant P^*, (5) is simply the statement that the increase in strain energy stored in the system must equal the work done by the lateral load for each unit length of propagation.

A numerical solution for the entire buckled shape of the beam is shown in Fig. 3.3, for the example, where

$$k(w) = k_0[1 - 4.5(w/H) + 5.25(w/H)^2], \tag{6}$$

where H can be thought of as the distance between the undeflected beam and the foundation base. The force–deflection curve from (6) is plotted in Fig. 3.1. The curve with $\rho c^2 = 0$ in Fig. 3.3 applies to the present quasi-static limit, while the curves for $\rho c^2 \neq 0$ involve inertial effects and will be discussed in a later section. The solution method for obtaining $w(x)$ is given in Section 3.6. In Fig. 3.3, $w(x)$ has been shifted so that $w(0) = (w_A + w_B)/2$.

3.3 Quasi-static spread of a buckle from a weak spot on the foundation

To illustrate the development of a propagating buckle, we take the unloaded beam to be straight but we assume the elastic foundation has variable stiffness according to

$$k(w, x) = k_0[1 - 4.5(w/H) + 5.25(w/H)^2](1 - \eta\, e^{-\lambda\xi^2}), \tag{7}$$

where $\xi = x(k_0/EI)^{1/4}$. With $\eta > 0$, the foundation is weakest near the

Fig. 3.3. Buckling mode profiles for steady-state propagation.

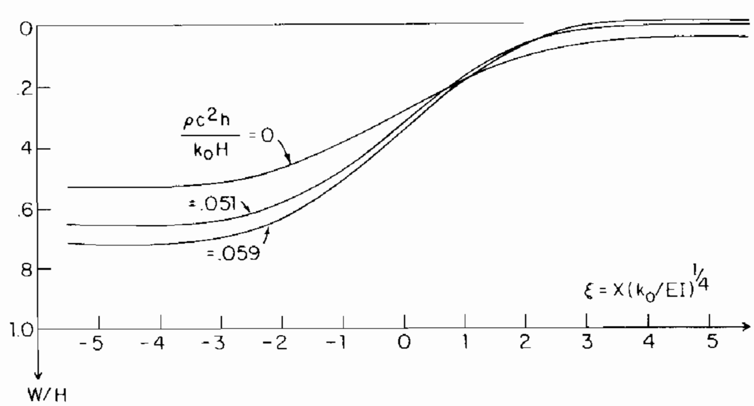

origin and it develops its full strength for $\lambda\xi^2 \gg 1$. As the uniform load per unit length P is increased from zero, the beam undergoes its largest deflection at the origin and this is the first section of the beam to experience collapse. A plot of a sequence of deflections is shown in Fig. 3.4 along with associated values of P. The load is normalized by P^*, the steady-state propagation load of the unweakened foundation. The deflections in Fig. 3.4 illustrate the case where $\eta = .2$ and $\lambda = 1/6$, which corresponds to a weakened region whose half-length is about the width of the transition zone of the steady-state shape in Fig. 3.3. The least deflected configuration in Fig. 3.4 corresponds to $P/P^* = 1.46$ which is just below the maximum load the weakened beam can support. After the peak load is achieved the buckle localizes under falling load until complete collapse occurs in the vicinity of $x = 0$. This part of the process has features in common with the localization of buckling modes as discussed by Tvergaard & Needleman (1980). But with further deflection the foundation stiffens up again in the vicinity of the origin and the stage is set for the buckle to spread. It can be seen in Fig. 3.4 that the buckle attains the steady-state profile as it spreads and it does so with P approaching P^*.

The spread and approach to steady-state is displayed in another way in Fig. 3.5 where the load is plotted as a function of the point $x = L$,

Fig. 3.4. Quasi-static buckle growth and spread for a foundation weakened near the origin ($\eta = .2$, $\lambda = 1/6$).

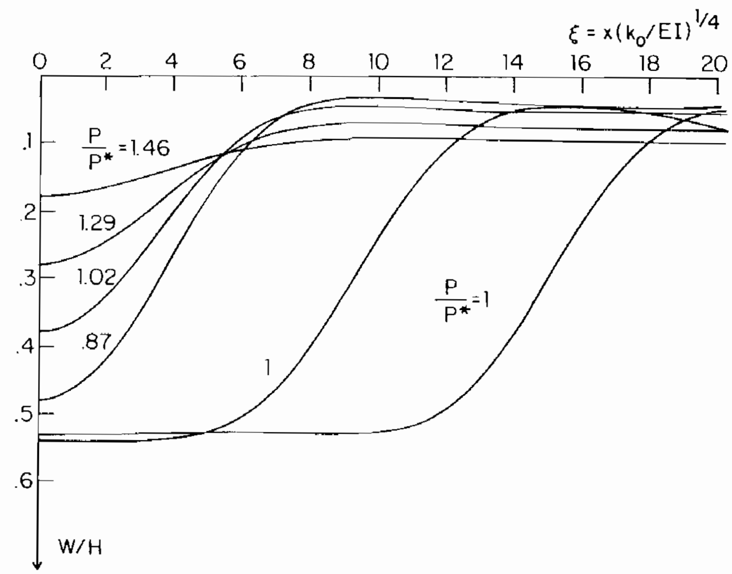

where the deflection attains the value associated with the local peak load of the foundation. For the foundation described by (7) the peak occurs at $w/H = .15$ for all x. Curves are shown for three levels of η with $\lambda = 1/6$ in each case. The intercept with the ordinate in Fig. 3.5 corresponds to the load when the deflection at the origin first attains $w/H = .15$. The curve for $\eta = .2$ can be compared with the deflection profiles in Fig. 3.4. The buckle starts to spread as the load rises above the local minimum at $P/P^* \approx .87$ when $L(k_0/EI)^{1/4} \approx 5$. As the buckle propagates, the load level quickly approaches the steady-state load P^*.

If the foundation is sufficiently weakened near $x = 0$, as it is in the case $\eta = .7$, the load approaches P^* from below. For smaller η a load greater than P^* is needed to initiate the spreading process. Of course, if the loading P is prescribed as a dead load, the portion of the deflection history in which the load is falling is unstable. At any local maximum of the load history the buckle would start to run dynamically. For either of the examples with $\eta = .2$ and .4 in Fig. 3.5, the buckle would not arrest if the load was held at the maximum value. However, in the case of the foundation which is weakened most at the origin ($\eta = .7$), the buckle would arrest since the load needed to initiate spreading is below P^*.

Fig. 3.5. Quasi-static spread of buckle for three levels of local foundation weakness ($\lambda = 1/6$).

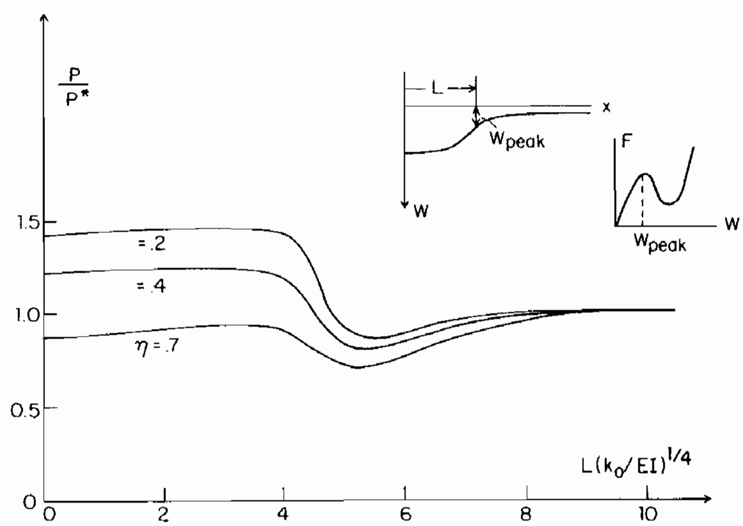

3.4 Dynamic steady-state propagation

We now reconsider steady-state propagation by including the inertia of the beam and inertial flow of an incompressible fluid which is imagined to be contained between the beam and the base of the foundation. As will be seen, the beam inertia itself does not affect the steady-state propagation load but the fluid does. The fluid is intended to give some insight into the effect which fluid in a pipe has on the propagation process.

The fluid flow is modeled as being quasi-one-dimensional with a single horizontal velocity component v taken to be positive in the positive x-direction. We consider steady-state buckle propagation where the deflection is of the form $w(x-ct)$ where t is time and c is the velocity of propagation. As in Fig. 3.1, the beam is imagined to have collapsed behind the transition and the buckle travels in the positive x-direction ($c>0$) into the uncollapsed region. By continuity, the velocity of the fluid at any point along the beam in this steady-state problem must satisfy

$$(v-c)(H-w) = \text{const} = -c(H-w_A). \tag{8}$$

We have taken the 'pipe' to be blocked well ahead of the buckle so that $v \to v_A = 0$ as $x \to +\infty$. Bernoulli's equation supplies the pressure p in the fluid. It is assumed that far behind the buckle as $x \to -\infty$ the 'pipe' is vented to a pressure p_B. Thus at any point along the beam

$$p + \tfrac{1}{2}\rho(v-c)^2 = p_B + \tfrac{1}{2}\rho(v_B - c)^2, \tag{9}$$

where ρ is the density of the fluid.

The equation governing the deflection of the beam is

$$EIw'''' + k(w)w = P - ph - mc^2 w'', \tag{10}$$

where $(\ )'$ denotes the derivative of $w(x-ct)$ with respect to its argument. Here m is the mass per unit length of the beam and h is its thickness in the direction perpendicular to the plane of Fig. 3.1. Since the exit pressure p_B can be absorbed in P by subtracting off $p_B h$, we will take $p_B = 0$ without any loss in generality.

Assuming as before that the derivatives of w vanish as $x \to \pm\infty$, the equilibrium conditions far ahead and behind the transition region are

$$P - p_A h = k(w_A)w_A \quad \text{and} \quad P = k(w_B)w_B, \tag{11}$$

with

$$(v_B - c)(H - w_B) = -c(H - w_A) \tag{12}$$

and

$$p_A + \tfrac{1}{2}\rho c^2 = \tfrac{1}{2}\rho(v_B - c)^2. \tag{13}$$

A fifth equation linking P, w_A, w_B, p_A and v_B is obtained by multiplying (10) by w' and integrating from $-\infty$ to $+\infty$, as in the quasi-static case, with the result

$$\int_{w_A}^{w_B} k(w)w\,dw + \tfrac{1}{2}\rho h(v_B - c)^2 \frac{(w_B - w_A)^2}{H - w_A} = P(w_B - w_A). \qquad (14)$$

That the inertia of the beam does not enter into the steady-state energy balance (14) is easily understood since the total kinetic energy associated with a translating profile $w(x-t)$ does not change with time. Thus, if the inertia of the fluid is neglected ($\rho = 0$), the graphical construction of Fig. 3.2 still pertains and P^* is independent of c, although the shape of the propagating buckle does depend on mc^2 through (10).

Suppose c is regarded as being specified. Then (11)–(14) provide five equations for the unknowns P, w_A, w_B, p_A and v_B. As $\rho c^2 \to 0$ the quasi-static solution is retrieved with $P = P^*$. Expanding the solution to (11)–(14) about the quasi-static solution for small ρc^2 gives

$$P = P^* + \tfrac{1}{2}\rho c^2 h \frac{(w_B^* - w_A^*)(H - w_A^*)}{(H - w_B^*)^2} + 0(\rho c^2)^2, \qquad (15)$$

where w_A^* and w_B^* denote values at the limit $\rho c^2 = 0$. A numerical example is given in Fig. 3.6 for the foundation law (6). The relation between P/P^* and $\rho c^2 h/(k_0 H)$ is plotted over the range between $\rho c^2 = 0$

Fig. 3.6. Load for dynamic steady-state buckle propagation.

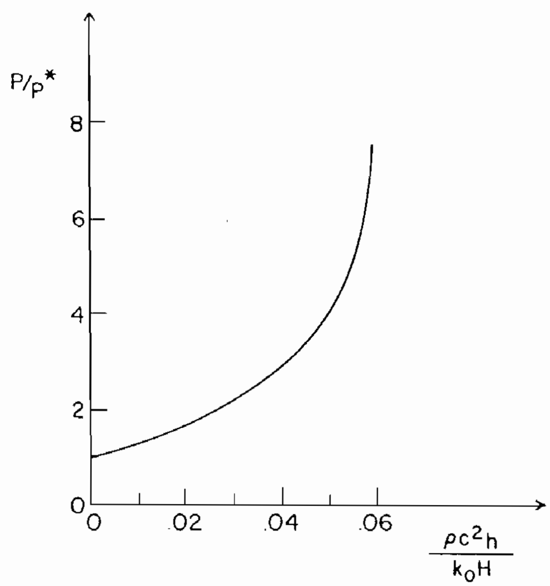

and the right limit where the curve has a vertical tangent. Buckle shapes are shown in Fig. 3.3 for two values of $\rho c^2 h/(k_0 H)$ along with the profile previously presented for the quasi-static case. For the two dynamic examples the additional nondimensional parameter was specified to be

$$\frac{mH}{\rho h}\left(\frac{k_0}{EI}\right)^{1/2}=1,$$

although additional calculations indicated that the shapes have relatively little dependence on this parameter over the range from 0 to 10.

3.5 Discussion

As long as the load is below the quasi-static propagation load P^*, no buckle can run the full length of the structure. If the load exceeds P^* then a buckle may run the full length of the structure if an initial disturbance or imperfection of sufficient magnitude can set off the process. The buckling behavior of the perfect structure involves the attainment of a limit load ($P = F_{max}$) and this type of buckling is only weakly imperfection-sensitive. In other words, it does take a fairly substantial *local* imperfection or disturbance to initiate a propagating buckle when the structure is loaded to P^* or just above. Nevertheless, if a local collapse can be repaired or tolerated while a complete running collapse is untenable, then P^* may be significant for structural design.

Acknowledgements

The work of E.C. was supported in part by the Natural Sciences and Engineering Research Council of Canada and by the National Science Foundation under Grant CME-78-10756. The work of J.W.H. was supported in part by the National Science Foundation under Grant CME-78-10756 and by the Division of Applied Sciences, Harvard University.

3.6 Appendix

The numerical method used in solving for $w(x)$ for the steady-state problem will be illustrated using the quasi-static case governed by (1). First, (1) is rewritten as

$$\frac{d^4 w}{d\xi^4}+w=U(w), \tag{16}$$

where

$$\xi = x(k_0/EI)^{1/4} \quad \text{and} \quad U(w)=\frac{1}{k_0}\{P+[k_0-k(w)]w\}. \tag{17}$$

An integral equation for w can be written as

$$w(\xi) = \int_{-\infty}^{\infty} G(\xi - t) U[w(t)]\, dt, \tag{18}$$

where the Green's function is

$$G(\xi) = \frac{1}{2\sqrt{2}} e^{-|\xi|/\sqrt{2}} [\sin(|\xi|/\sqrt{2}) + \cos(\xi/\sqrt{2})]. \tag{19}$$

A change of variable is made according to

$$z = \tanh \frac{1}{\sqrt{2}} \xi \quad \left.\begin{matrix} -\infty \leq \xi < \infty \\ -1 \leq z \leq 1. \end{matrix}\right\} \tag{20}$$

Then an approximation to w in terms of the new variable is written as

$$w(z) = \tfrac{1}{2}(w_A + w_B) + \tfrac{1}{2}(w_A - w_B)z + \sum_{n=1}^{N} (A_n \cos \lambda_n z + B_n \sin \mu_n z), \tag{21}$$

where $\lambda_n = (2n-1)\pi/2$ and $\mu_n = n\pi$. To render the solution unique, we require $w(0) = (w_A + w_B)/2$ so that the following constraint must hold:

$$\sum_{n=1}^{N} A_n = 0. \tag{22}$$

The $2N$ free parameters, A_n and B_n, in (21) were determined by satisfying (18) at $2N-1$ values of z and by meeting the constraint (22). The integration in (18) was carried out using Gaussian quadrature. Since (18) is nonlinear in the free parameters, Newton–Raphson iteration was used to compute the solution. A convergence study based on increasing N revealed that the choice $N = 6$ gave results for w which are accurate to about three significant figures.

The above approach could have been adapted to the analysis of the spreading process for the initially imperfect system, but we found it simpler to use a direct two-point finite difference integration scheme applied to the incremental problem. The infinite beam was approximated by a finite beam of length $2l$, where $l = 60\ (EI/k_0)^{1/4}$, corresponding to about ten times the length of the transition region of the steady-state mode shape. At low loads, increments of P were prescribed. But as P approached a peak, a switch to the most rapidly changing displacement value was made for use as the prescribed incremental quantity.

References

James, R. D. (1979). 'Co-existent phases in the one-dimensional static theory of elastic bars'. *Archive for Rational Mechanics and Analysis*, **72**, 99–140.

Kyriakides, S. & Babcock, C. D. (1980). *The Propagating Buckle in Marine Pipelines*. Final Report to The American Petroleum Institute, Aeronautical Laboratories, California Institute of Technology, Pasadena, California.

Kyriakides, S. & Babcock, C. D. (1981). 'Large deflection collapse analysis of an inelastic inextensional ring under external pressure'. *International Journal of Solids and Structures*, **17**, 981–93.

Maxwell, J. C. (1875). 'On the dynamical evidence of the molecular constitution of bodies'. *Nature*, **11**, 357.

Palmer, A. C. & Martin, J. H. (1975). 'Buckle propagation in submarine pipelines'. *Nature*, **254**, 46–8.

Tvergaard, V. & Needleman, A. (1980). 'On the localization of buckling problems'. *Journal of Applied Mechanics*, **47**, 613–19.